ChemComm

COMMUNICATION

View Article Online
View Journal | View Issue

Cite this: *Chem. Commun.*, 2019, 55, 182

Received 28th October 2018,
Accepted 30th November 2018

DOI: 10.1039/c8cc08618d

rsc.li/chemcomm

Synthesis and biochemical characterization of quasi-stable trimer models of full-length amyloid β40 with a toxic conformation†

Yumi Irie,[a] Mizuho Hanaki,[a] Kazuma Murakami,[a] Tsuneo Imamoto,[b] Takumi Furuta,[c] Takeo Kawabata,[c] Taiji Kawase,[d] Kenji Hirose,[d] Yoko Monobe,[e] Ken-ichi Akagi,[e] Ryo C. Yanagita[f] and Kazuhiro Irie*[a]

Here, we report the first synthesis of quasi-stable trimer models of full-length Aβ40 with a toxic conformation using a 1,3,5-phenyltris-L-alanyl linker at position 34, 36, or 38. The only trimer to exhibit weak neurotoxicity against SH-SY5Y cells was the one which was linked at position 38. This suggests that such a propeller-type trimer model is not prone to forming oligomers with potent neurotoxicity, which is in contrast with its corresponding dimer model.

Amyloid β proteins are peptides of 36–43 amino acids in length (Aβ36–Aβ43) found in senile plaques[1,2] that are involved in the pathogenesis of Alzheimer's disease (AD).[3,4] Oligomeric assemblies of Aβ could induce synaptotoxicity during AD progression.[5] Aβ42 is the protein which is most prone to aggregation and to forming toxic oligomers as well as less-toxic fibrils, but the oligomers of Aβ40 can also become neurotoxic as demonstrated by the dimer models of Aβ40.[6–9] "Aggregation" in this paper is defined as the change of Aβ monomers into oligomers, protofibrils, or amyloid fibrils. It is quite difficult to determine the mechanism of toxicity of Aβ oligomers since the aggregation speed of Aβ monomers is very fast. The oligomeric state could not easily be captured even when using ion mobility-mass spectrometry (IM-MS).[10,11] To overcome this difficulty, various dimer models of Aβ have been synthesized and characterized.[6–9,12,13] These studies identified the important residues involved in the oligomerization and fibrillization processes. As shown by Teplow's pioneering studies to capture oligomeric states of Aβ, photochemically cross-linked Aβ oligomers have also been prepared and were found to be neurotoxic, but the cross-linking positions were not limited to one residue.[14–17]

We have recently synthesized quasi-stable dimers of E22P–Aβ40 and E22P–Aβ42 with an L,L-2,6-diaminopimeric acid (DAP) linker at positions 38 and 40, respectively, and in doing so, have demonstrated that the formation of the C-terminal hydrophobic core is necessary to form toxic oligomers.[9,18] Since the E22P mutation could accelerate the formation of the toxic oligomers,[19–21] we named the turn structure at positions 22 and 23 the "toxic turn". These two dimer models existed as quasi-stable oligomers, and exhibited potent neurotoxicity against SH-SY5Y cells.[9,18] Although oligomers derived from Aβ dimers could be involved in the pathogenesis of AD,[22–24] several reports have suggested that Aβ trimers as well as Aβ dimers could also contribute to its onset.[25,26] Recently, the synthesis of trimer models of Aβ fragments has been reported and characterized,[27,28] however, there are no reports describing the synthesis of full-length Aβ trimer models. In this paper, we report the first synthesis and biochemical characterization of quasi-stable trimer models of full-length Aβ40 with a toxic conformation using a 1,3,5-phenyltris-L-alanyl linker (Fig. 1A) at position 34, 36, or 38 (**7–9** in Fig. 1C). Our goal in doing this was to use these models to investigate whether the dimers or trimers are more relevant to AD progression by comparing the E22P–Aβ40 dimer model with a DAP linker at position 38 (**10**). We selected E22P–Aβ40 as a template for the full-length trimer because the aggregative ability and neurotoxicity of wild-type Aβ40 are much lower than those of E22P–Aβ40.[29]

We adopted a 1,3,5-phenyltris-L-alanyl linker for the trimer synthesis since this linker enables the formation of anti-parallel β-sheets at the C-terminal region, which exists in one of the proposed trimer models by Huang *et al.* using solid-state NMR [Fig. 1B(i, ii)].[30] A molecular modelling study indicated that the V36 core region of this trimer model is reproducible by linking position 36 with the 1,3,5-phenyltris-L-alanyl linker [Fig. 1B(iii)]. We therefore synthesized (*S*,*S*,*S*)-Fmoc-1,3,5-phenyltris-L-alanine to be used in solid-phase synthesis as one amino acid residue

[a] *Division of Food Science and Biotechnology, Graduate School of Agriculture, Kyoto University, Kyoto 606-8502, Japan. E-mail: irie@kais.kyoto-u.ac.jp; Fax: +81-75-753-6284; Tel: +81-75-753-6281*
[b] *Nippon Chemical Industrial Co. Ltd, Tokyo 136-8515, Japan*
[c] *Institute for Chemical Research, Kyoto University, Kyoto 611-0011, Japan*
[d] *Nihon Waters K. K., Tokyo 140-0001, Japan*
[e] *National Institute of Biomedical Innovation, Health and Nutrition, Osaka 567-0085, Japan*
[f] *Department of Applied Biological Science, Faculty of Agriculture, Kagawa University, Kagawa 761-0795, Japan*

† Electronic supplementary information (ESI) available: Experimental procedures and Fig. S1–S3. See DOI: 10.1039/c8cc08618d

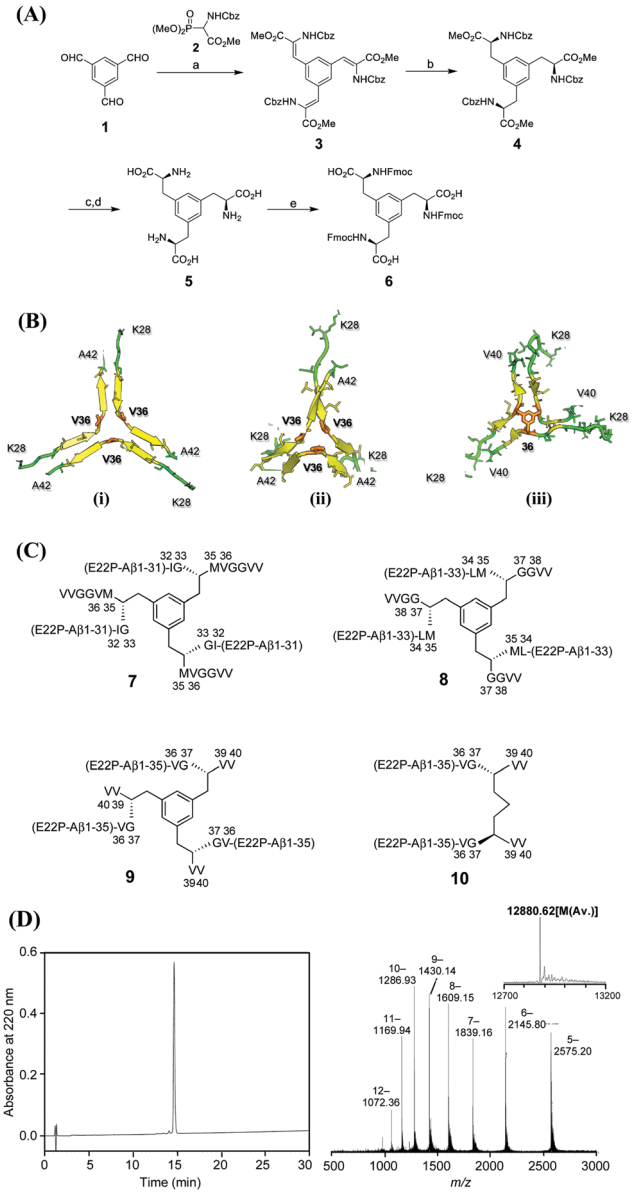

Fig. 1 (A) Synthesis of (*S*,*S*,*S*)-Fmoc-1,3,5-phenyltris-L-alanine: (a) 1,1,3,3-tetramethyl guanidine, THF, 0 °C to rt, 4 h, 76%. (b) Rh-(*S*,*S*)-QuinoxP,[32] H_2 (4 atm), EtOAc/MeOH, rt, 4 h, 92% (>98%ee, >98%de). (c) NaOHaq, MeOH, 1 h, 97%. (d) H_2, Pd/C, MeOH, overnight, 75%. (e) Fmoc-OSu, Na_2CO_3, MeCN, H_2O, 3 d, 50%. (B) (i) Idealized trimer model in the C-terminal region (K28–A42) of wild-type Aβ42 based on solid-phase NMR proposed by Huang *et al.*[30] (ii) Snapshot of the Aβ42 trimer model in the C-terminal region after 1 ns of molecular dynamics simulation. (iii) The C-terminal region of the trimer model **8** with the 1,3,5-phenyltris-L-alanyl linker at position 36; the snapshot was extracted after 1 ns of molecular dynamics simulation. In A–C, ribbons represent anti-parallel β-strands, and V36 and the phenyl linker residues are represented in stick models and coloured orange. For clarity, nonpolar hydrogen atoms are not displayed. (C) Structure of the trimer models synthesized in this study (**7–9**) along with the dimer model (**10**).[9] (D) HPLC profile and ESI-qTOF-MS data with deconvolution of the trimer model **8** as a representative example. HPLC condition: X-bridge (100 × 4.6 mm I.D.), 1 mL min^{-1}, UV 220 nm, 20–50% acetonitrile containing 0.1% trifluoroacetic acid (30 min linear gradient), 10 μg/10 μL (0.15% NH_4OH) injection. **8**, *m/z* 12880.62 (calcd for av. mass, 12881.58).

at position 34, 36, or 38. The synthesis started with 1,3,5-triformylbenzene (**1**) according to previously reported methods,[31] with modifications (Fig. 1A). Horner–Wadsworth–Emmons olefination of **1** gave **3**, whose stereochemistry (all-*Z*) was confirmed by the NOESY spectrum.

Asymmetric hydrogenation of **3** using Rh-(*S*,*S*)-QuinoxP[32] gave **4** with a 92% yield. The diastereomeric ratio and enantiomeric excess of **4**, after purification using a silica-gel column, were determined to be >98% (Fig. S1 in ESI†). Alkaline hydrolysis of **4**, followed by deprotection, gave **5**, whose amino groups were protected with Fmoc. The overall yield of the linker **6** was 25%.

The three trimer models of E22P–Aβ40 with the linker **6** at position 34, 36, or 38 (**7–9**, Fig. 1C) were synthesized in a stepwise fashion on preloaded Fmoc-L-Val-PEG-PS resin by a microwave peptide synthesizer (ESI†). Each coupling reaction was carried out using each Fmoc amino acid, HATU,[33] and *N*,*N*-diisopropylethylamine in DMF. The 1/3 molar equivalent trimer linker **6** (0.033 mmol) was employed instead of Fmoc-L-Leu, Fmoc-L-Val, or Fmoc-Gly at position 34, 36, or 38, respectively, in order to avoid formation of the mono-coupled and/or di-coupled peptides. This procedure gave **7–9** at yields of 0.58%, 1.1%, and 0.45%, respectively, after HPLC purification using C_4 and C_{18} columns under acidic conditions (ESI†). Their purity was checked by HPLC analysis, and their molecular weights and formulae were confirmed by ESI-qTOF-MS measurements (Fig. S2 in ESI†). Only the data of **8** are shown in Fig. 1D as a representative example.

The aggregative ability of the trimer models (**7–9**) was evaluated using thioflavin-T (Th-T) that fluoresces when bound to the β-sheet structure in Aβ aggregates (Fig. 2A).[34] Unlike wild-type Aβ40,[29] E22P–Aβ40 with the toxic turn promptly aggregated to give a high level of fluorescence. In contrast, the fluorescence intensity of **7–9** was weaker than that of E22P–Aβ40 for two weeks, suggesting that these trimer models did not form typical fibrils like E22P–Aβ40. This was confirmed by transmission electron microscopy (TEM) analysis (Fig. 2B). Only small amounts of amorphous aggregates were detected for **7** and **8**, while **9** and **10** formed protofibrils (fibrils) after 48 h. E22P–Aβ40 showed the highest fluorescence intensity among them. The fluorescence intensity in the Th-T assay was different among E22P–Aβ40, **9**, and **10**; this might reflect the number of fibrils and their structural differences.

Furthermore, time-dependent circular dichroism (CD) measurements were conducted (Fig. 2C). E22P–Aβ40 exhibited a positive peak at *ca.* 195 nm and a negative peak at *ca.* 215 nm after 4 h incubation, indicating the formation of the β-sheet structure. In contrast, the secondary structures of **7** and **8** remained almost random even after 48 h incubation. The trimer **9** with the linker **6** at position 38 formed a β-sheet rich structure in a time-dependent manner. Consistently, the TEM analyses after 48 h incubation (Fig. 2B) showed that only **9** formed protofibrils (fibrils).

We then measured the neurotoxicity of **7–9** against SH-SY5Y cells (human neuroblastoma) using the MTT [(4,5-dimethylthiazol-2-yl)-2,5-diphenyltetrazolium bromide] assay (Fig. 3A). After incubation for 16 h with each compound at various concentrations, cell viability was estimated by the ability to reduce MTT. The dimer model **10** significantly decreased cell viability even at 1 μM. Among the trimer models (**7–9**), only **9** exhibited weak neurotoxicity through somewhat decreased cell viability.

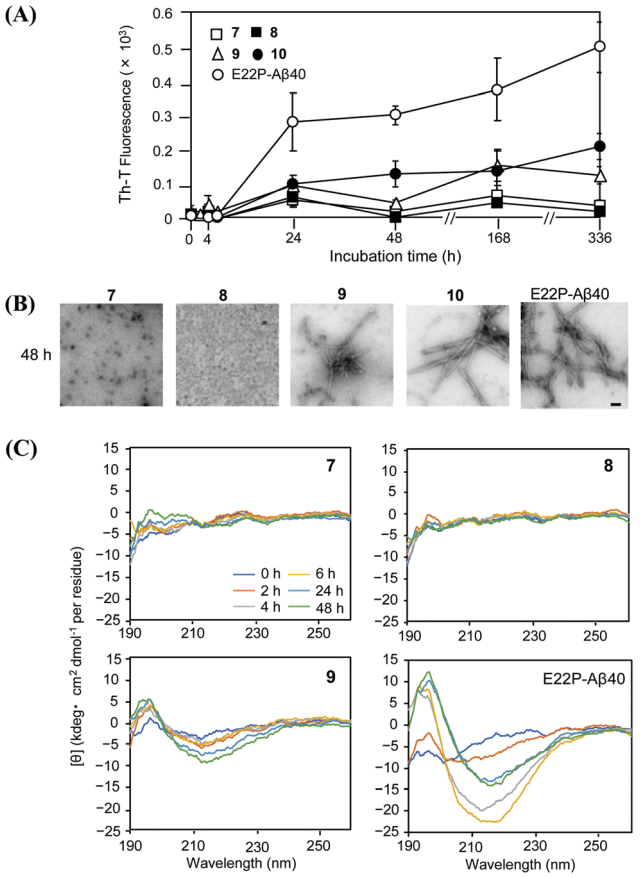

Fig. 2 (A) Th-T fluorescence of the trimer models **7–9** (8 μM) along with that of E22P–Aβ40 (25 μM) and the dimer model **10** (12.5 μM) after the indicated incubation times at 37 °C. Data are expressed as mean ± SD (n = 8). (B) TEM analyses of the aggregates of **7–10**, and E22P–Aβ40 (8, 12.5, or 25 μM) after 48 h incubation at 37 °C. Scale bar = 50 nm (magnification: 30 k). (C) CD spectra of **7–9** (8 μM) and E22P–Aβ40 (25 μM) after incubation for the indicated duration at 37 °C.

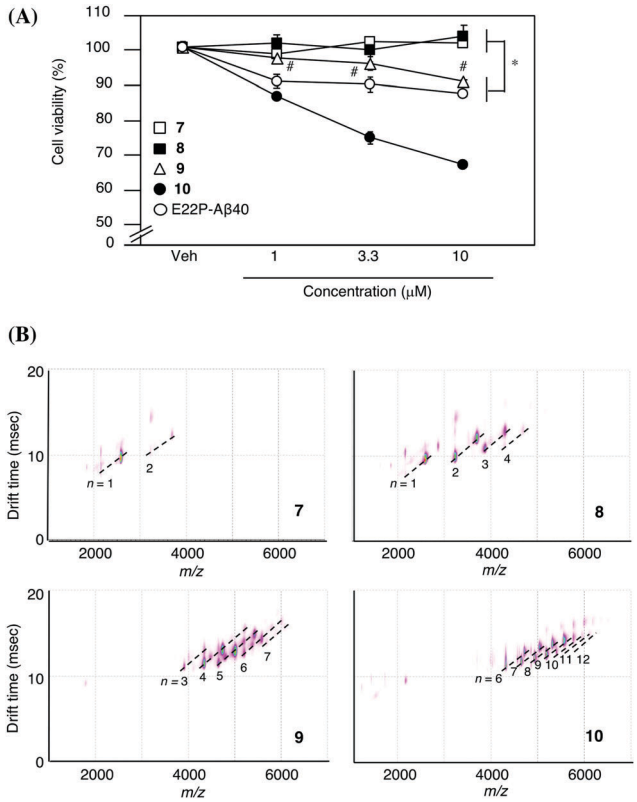

Fig. 3 (A) Neurotoxicity against SH-SY5Y of the trimer models **7–9** along with that of E22P–Aβ40 monomer and the dimer model **10** after 16 h incubation at 37 °C. Absorbance obtained after adding vehicle (0.15% NH_4OH) was taken as 100%. *p < 0.05, #p < 0.05 *versus* vehicle. (B) IM-MS of **7–9** (8 μM) along with **10** (12.5 μM) after 4 h incubation at 37 °C. "n" denotes an integer corresponding to the number of units coexisting in the solution depending on their drift time.

Finally, in order to determine the size of the oligomers ascribable to the neurotoxicity, measurements were conducted using IM–MS combined with nanoelectrospray. Since IM–MS after 2, 4, and 6 h incubation was similar in each trimer model, only the 2D heat maps with m/z and drift time after 4 h incubation were shown in Fig. 3B. Their projection of the 2D spectra on the mass spectra axis is shown in Fig. S3 in ESI.† After deconvolution based on the observed and calculated masses, cross-peaks were assigned to the series of multivalent ions (n = 1, 2, 3… of each trimer model denotes trimer, hexamer, nonamer, …, respectively). As a control, the dimer model **10** with a DAP linker at position 38 formed higher-order oligomers (n = 6–12 : 12–24-mer), and the E22P–Aβ40 monomer did not give any cross peaks because of high aggregation velocity (data not shown). Trimer **7** with the linker at position 34 did not form oligomers; it remained a trimer and hexamer (n = 1–2) even after 24 h of incubation (data not shown). In contrast, **8** existed as a 3–12-mer (n = 1–4), and **9** formed larger oligomers of 9–21 mer (n = 3–7). It should be stated that it remains unclear if the distinct toxicities of the Aβ40 trimers are due to differences in oligomer size, or due to other consequences of the different chemistries of the models, for example, the extent of oligomer/fibril formation, oligomer/fibril structure, or distinct oligomer/fibril surface chemistry. These issues may be clarified by further studies on the structural basis of these models using NMR and cryo-EM.

To the best of our knowledge, this is the first report on the synthesis and biochemical characterization of the full-length trimer model based on the trimer structure in Aβ42 oligomers (150 kDa, *ca.* 30-mer) deduced from solid-state NMR.[30] This trimer model with the linker at position 36 (**8**) was quasi-stable, but its neurotoxicity was very weak compared with the dimer and the trimer models with the linkers at position 38 (**10** and **9**). These data suggest that the position of the C-terminal hydrophobic core could influence the toxicity of Aβ oligomers, and that at least the propeller-like trimer model **9** is not prone to form oligomers with potent neurotoxicity, which is in contrast with its corresponding dimer model **10**. Although the trimer models in this study reference the Aβ40 protein, the C-terminal hydrophobic interaction in the Aβ42 dimer could partly be mimicked by the Aβ40 dimer model *via* the covalent linkage at the C-terminal region; in fact, the neurotoxicities of the dimer models of Aβ40 and Aβ42 with the DAP linker at

positions 38 and 40, respectively, were quite similar to each other.[9,18]

In summary, we have synthesized three full-length trimer models, **7–9**, with toxic conformations. The linker **6** was selected to reproduce the putative trimer structure of Aβ42 oligomers.[30] The synthesis of these models is straightforward and practical although the purification step involves some laborious operations. Only **9**, with the linker at position 38, formed larger oligomers of 9–21-mer that were weakly neurotoxic against SH-SY5Y cell lines. Therefore, the trimer model **9** as well as the dimer model **10** may be useful tools to understand amyloid aggregation and how the aggregates correlates to toxicity.

Notably, as the neurotoxicities of **7–9** did not exceed that of the monomer and the dimer model **10**, which has an intermolecular parallel β-sheet, these propeller-type trimer models with an anti-parallel β-sheet at the C-terminal region by the linker **6** may not reflect the structure of toxic Aβ oligomers. Alternatively, Aβ dimers like **10** might play a more critical role in the pathogenesis of AD compared with the propeller-type trimers. In order to verify which is more important, further attempts to synthesize other types of trimer models, for example trimers with intermolecular parallel β-sheets similar to the dimer model **10**, are required. Synthesis of the corresponding 42-mer models would also be necessary.

It is quite difficult to determine the mechanism of toxicity of Aβ oligomers since the aggregation speed of Aβ monomers is very fast. In particular, while this is true for *in vivo* conditions, studies have shown the mechanisms of toxicity *via* membrane disruption and two steps of pore formation *versus* fiber-dependent detergent-like mechanisms.[35] Since synthetic oligomers do not always reflect the heterogeneous mixture present *in vivo*, the dynamics (or mobility) of residues that may be responsible for toxicity could be different for synthetic species. In addition, their affinity for the cell membrane and its disruption could also be different.

This work was supported by JSPS KAKENHI Grant Number 26221202 to K. I. and K. M. The authors thank Ms Tomoyo Takai and Ms Ritsuko Yamaguchi at the National Institute of Biomedical Innovation for their assistance with TEM analysis.

Conflicts of interest

There are no conflicts to declare.

Notes and references

1 G. G. Glenner and C. W. Wong, *Biochem. Biophys. Res. Commun.*, 1984, **120**, 885–890.
2 C. L. Masters, G. Simms, N. A. Weinman, G. Multhaup, B. L. McDonald and K. Beyreuther, *Proc. Natl. Acad. Sci. U. S. A.*, 1985, **82**, 4245–4249.
3 J. A. Hardy and G. A. Higgins, *Science*, 1992, **256**, 184–185.
4 J. Hardy and D. J. Selkoe, *Science*, 2002, **297**, 353–356.
5 D. M. Walsh, I. Klyubin, J. V. Fadeeva, W. K. Cullen, R. Anwyl, M. S. Wolfe, M. J. Rowan and D. J. Selkoe, *Nature*, 2002, **416**, 535–539.
6 B. O'Nuallain, D. B. Freir, A. J. Nicoll, E. Risse, N. Ferguson, C. E. Herron, J. Collinge and D. M. Walsh, *J. Neurosci.*, 2010, **30**, 14411–14419.
7 W. M. Kok, J. M. Cottam, G. D. Ciccotosto, L. A. Miles, J. A. Karas, D. B. Scanlon, B. R. Roberts, M. W. Parker, R. Cappai, K. J. Barnham and C. A. Hutton, *Chem. Sci.*, 2013, **4**, 4449–4454.
8 T. T. O'Malley, N. A. Oktaviani, D. Zhang, A. Lomakin, B. O'Nuallain, S. Linse, G. B. Benedek, M. J. Rowan, F. A. A. Mulder and D. M. Walsh, *Biochem. J.*, 2014, **461**, 413–426.
9 Y. Irie, K. Murakami, M. Hanaki, Y. Hanaki, T. Suzuki, Y. Monobe, T. Takai, K.-i. Akagi, T. Kawase, K. Hirose and K. Irie, *ACS Chem. Neurosci.*, 2017, **8**, 807–816.
10 S. L. Bernstein, N. F. Dupuis, N. D. Lazo, T. Wyttenbach, M. M. Condron, G. Bitan, D. B. Teplow, J. E. Shea, B. T. Ruotolo, C. V. Robinson and M. T. Bowers, *Nat. Chem.*, 2009, **1**, 326–331.
11 M. Kloniecki, A. Jablonowska, J. Poznanski, J. Langridge, C. Hughes, I. Campuzano, K. Giles and M. Dadlez, *J. Mol. Biol.*, 2011, **407**, 110–124.
12 W. M. Kok, D. B. Scanlon, J. A. Karas, L. A. Miles, D. J. Tew, M. W. Parker, K. J. Barnham and C. A. Hutton, *Chem. Commun.*, 2009, 6228–6230.
13 T. Yamaguchi, H. Yagi, Y. Goto, K. Matsuzaki and M. Hoshino, *Biochemistry*, 2010, **49**, 7100–7107.
14 G. Bitan, A. Lomakin and D. B. Teplow, *J. Biol. Chem.*, 2001, **276**, 35176–35184.
15 G. Bitan and D. B. Teplow, *Acc. Chem. Res.*, 2004, **37**, 357–364.
16 D. B. Teplow, N. D. Lazo, G. Bitan, S. Bernstein, T. Wyttenbach, M. T. Bowers, A. Baumketner, J.-E. Shea, B. Urbanc, L. Cruz, J. Borreguero and H. E. Stanley, *Acc. Chem. Res.*, 2006, **39**, 635–645.
17 G. Yamin, T.-P. V. Huynh and D. B. Teplow, *Biochemistry*, 2015, **54**, 5315–5321.
18 K. Murakami, M. Tokuda, T. Suzuki, Y. Irie, M. Hanaki, N. Izuo, Y. Monobe, K.-i. Akagi, R. Ishii, H. Tatebe, T. Tokuda, M. Maeda, T. Kume, T. Shimizu and K. Irie, *Sci. Rep.*, 2016, **6**, 29038.
19 A. Morimoto, K. Irie, K. Murakami, Y. Masuda, H. Ohigashi, M. Nagao, H. Fukuda, T. Shimizu and T. Shirasawa, *J. Biol. Chem.*, 2004, **279**, 52781–52788.
20 K. Murakami, K. Irie, H. Ohigashi, H. Hara, M. Nagao, T. Shimizu and T. Shirasawa, *J. Am. Chem. Soc.*, 2005, **127**, 15168–15174.
21 Y. Masuda, S. Uemura, R. Ohashi, A. Nakanishi, K. Takegoshi, T. Shimizu, T. Shirasawa and K. Irie, *ChemBioChem*, 2009, **10**, 287–295.
22 C. Lendel, M. Bjerring, A. Dubnovitsky, R. T. Kelly, A. Filippov, O. N. Antzutkin, N. C. Nielsen and T. Härd, *Angew. Chem., Int. Ed.*, 2014, **53**, 12756–12760.
23 I. Klyubin, V. Betts, A. T. Wetzel, K. Blennow, H. Zetterberg, A. Wallin, C. A. Lemere, W. K. Cullen, Y. Peng, T. Wisniewski, D. J. Selkoe, R. Anwyl, D. M. Walsh and M. J. Rowan, *J. Neurosci.*, 2008, **28**, 4231–4237.
24 G. M. Shankar, S. Li, T. H. Mehta, A. Garcia-Munoz, N. E. Shepardson, I. Smith, F. M. Brett, M. A. Farrell, M. J. Rowan, C. A. Lemere, C. M. Regan, D. M. Walsh, B. L. Sabatini and D. J. Selkoe, *Nat. Med.*, 2008, **14**, 837–842.
25 T. Tomiyama, T. Nagata, H. Shimada, R. Teraoka, A. Fukushima, H. Kanemitsu, H. Takuma, R. Kuwano, M. Imagawa, S. Ataka, Y. Wada, E. Yoshioka, T. Nishizaki, Y. Watanabe and H. Mori, *Ann. Neurol.*, 2008, **63**, 377–387.
26 M. Townsend, G. M. Shankar, T. Mehta, D. M. Walsh and D. J. Selkoe, *J. Physiol.*, 2006, **572**, 477–492.
27 R. K. Spencer, H. Li and J. S. Nowick, *J. Am. Chem. Soc.*, 2014, **136**, 5595–5598.
28 K. Shinoda, Y. Sohma and M. Kanai, *Bioorg. Med. Chem. Lett.*, 2015, **25**, 2976–2979.
29 K. Murakami, K. Irie, A. Morimoto, H. Ohigashi, M. Shindo, M. Nagao, T. Shimizu and T. Shirasawa, *J. Biol. Chem.*, 2003, **278**, 46179–46187.
30 D. Huang, M. I. Zimmerman, P. K. Martin, A. J. Nix, T. L. Rosenberry and A. K. Paravastu, *J. Mol. Biol.*, 2015, **427**, 2319–2328.
31 A. Ritzén, B. Basu, A. Wållberg and T. Frejd, *Tetrahedron: Asymmetry*, 1998, 3491–3496.
32 T. Imamoto, K. Tamura, Z. Zhang, Y. Horiuchi, M. Sugiya, K. Yoshida, A. Yanagisawa and I. D. Gridnev, *J. Am. Chem. Soc.*, 2012, **134**, 1754–1769.
33 L. A. Carpino, *J. Am. Chem. Soc.*, 1993, **115**, 4397–4398.
34 H. Naiki and F. Gejyo, *Methods Enzymol.*, 1999, **309**, 305–318.
35 S. A. Kotler, P. Walsh, J. R. Brender and A. Ramamoorthy, *Chem. Soc. Rev.*, 2014, **43**, 6692–6700.